doi.org/10.52568/001391/JCSP/45.06.2023

Design, Synthesis and Biological Evaluation of Several Novel 4-aminoquinazoline Derivatives as Potent Anti-Tumor Agents

[1]Liang-liang Chi, [1]Zhi-Qiang Cai*, [1]Bo Wang, [1]Wei-Tao Qin, [1]Ya-Nan Wang
[2]Qiao-Qiao Feng** and [3]Wen-Jie Ren
[1]*Liaoning Province Professional and Technical Innovation Center for Fine Chemical Engineering of Aromatics Downstream, School of Petrochemical Engineering, Shenyang University of Technology, Liaoyang, 111003, Liaoning, P. R. China.*
[2]*Shandong center for food and drug evaluation & inspection, 250101, Shandong, P. R. China.*
[3]*Key Laboratory for Chemical Drug Research of Shandong Province, Instiitute of Phamaceutical Sciences of Shandong Province, 250101, Shandong, P. R. China.*
kahongzqc@163.com*, czq0601@126.com**

(Received on 25th April 2022, accepted in revised form 1st December 2022)

Summary: A series of 4-aminoquinazoline derivatives were designed and synthesized as epidermal growth factor receptor (EGFR) inhibitors in our group. The bioassay results showed all the target compounds possessed potential anti-tumor activities against on A549 and H1975 cell lines. The IC_{50} values of 8.35 (for A549) and 19.18 μM (for H1975) exhibited remarkable inhibitory activity of compound **7d**, which were better compared to the positive control Afatinib (IC_{50} = 10.41 μM for A549, IC_{50} = 24.96 μM for H1975). In addition, the molecular docking and ADME prediction of compound **7d** was carried out. The experimental results show the compound **7d** is worth to further research and discuss.

Keywords: Quinazoline, Synthesis, Anti-tumor activity, Molecular docking, ADME.

Introduction

Quinazoline is a compound composed of benzene ring and pyrimidine ring. It is an alkaloid which is isolated from Chinese plant (dichroa febrifuga Lour) [1, 2]. Compounds containing quinazoline skeletons have been found to possess many pharmacological and biological activities, such as anti-inflammatory, anti-bacterial, anti-tuberculosis, anti-diabetic, anti-HIV and anti-tumor, etc [1-7]. As a key structure, quinazoline can produce a variety of biological activities in the field of anti-tumor agents [8-10] because it can connect different pharmacodynamic groups. Among many small molecule inhibitors, 4-aminoquinazoline has become the core skeleton of a variety of receptor tyrosine kinase inhibitors [11, 12], such as Zorifertinib (Fig. 1), which can cross the blood-brain barrier and has good CNS permeability. It is effective for treatment of tumours with brain metastasis [13]; Gefitinib (Fig. 1), which is approved by FDA for cancer treatment, can directly act on the ATP binding region of EGFR to inhibit the activity of EGFR; Afatinib (Fig. 1), which is the second-generation tyrosine kinase inhibitor of EGFR and HER2 with dual effective and irreversible [14-16], and it can covalently bind to HER2 and EGFR kinases and lead to irreversible inhibition in the treatment of non-small cell lung cancer. With the goal of finding more 4-aminoquinazoline based anti-tumor agents, all the target compounds **7a-7f** and **8a-8f** were designed and shown in Fig. 2, the active sites of quinazoline were modified respectively in this study. 4-position of quinazoline was substituted by different arylamino group, especially 3-ethynylphenyl-amino group and 3-chloro-4-fluoro phenylamino group, which have been widely utilized in designing many EGFR inhibitors, such as Gefitinib and Afatinib. Phenylamino with different substituted groups (such as 4-fluoro-2-methyl-phenylamino group, 2,4-dimethyl-phenylamino group, 4-methyl phenylamino groupa and 2-fluoro phenylamino group) were introduced at position of block 1 to adjust the binding modes between compounds and target protein. Isobutyryl and acryloyl were introduced at position of block 2, cyclohexyl and morpholine were introduced at position of block 3 to enhance the physicochemical properties and drug metabolism of the compounds [17]. And the *in vitro* anti-tumor activities of the designed compounds were tested by human lung adenocarcinoma cell lines A549 (with the overexpressed $EGFR^{WT}$) and H1975 (with the overexpressed $EGFR^{L858R/T790M}$). In addition, molecular docking analysis was also performed to seek the possible binding mode between the selected

*To whom all correspondence should be addressed.

compound and target protein of $EGFR^{WT}$ and $EGFR^{L858R/T790M}$ to analyze and discuss their action mode.

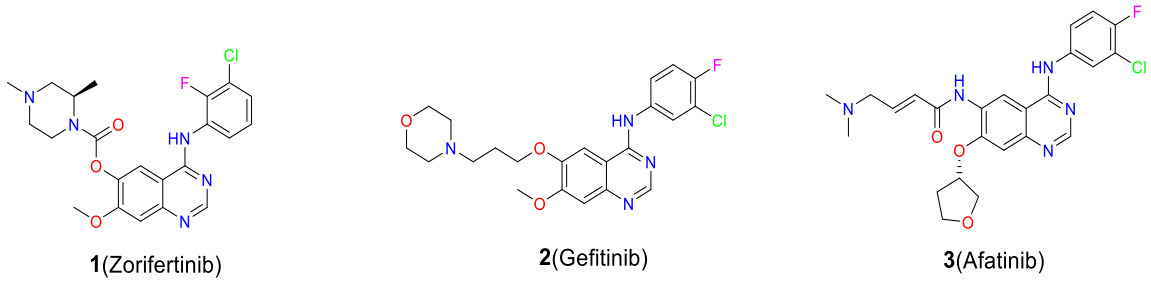

Fig. 1: The structures of 1(Zorifertinib), 2(Gefitinib) and 3(Afatinib).

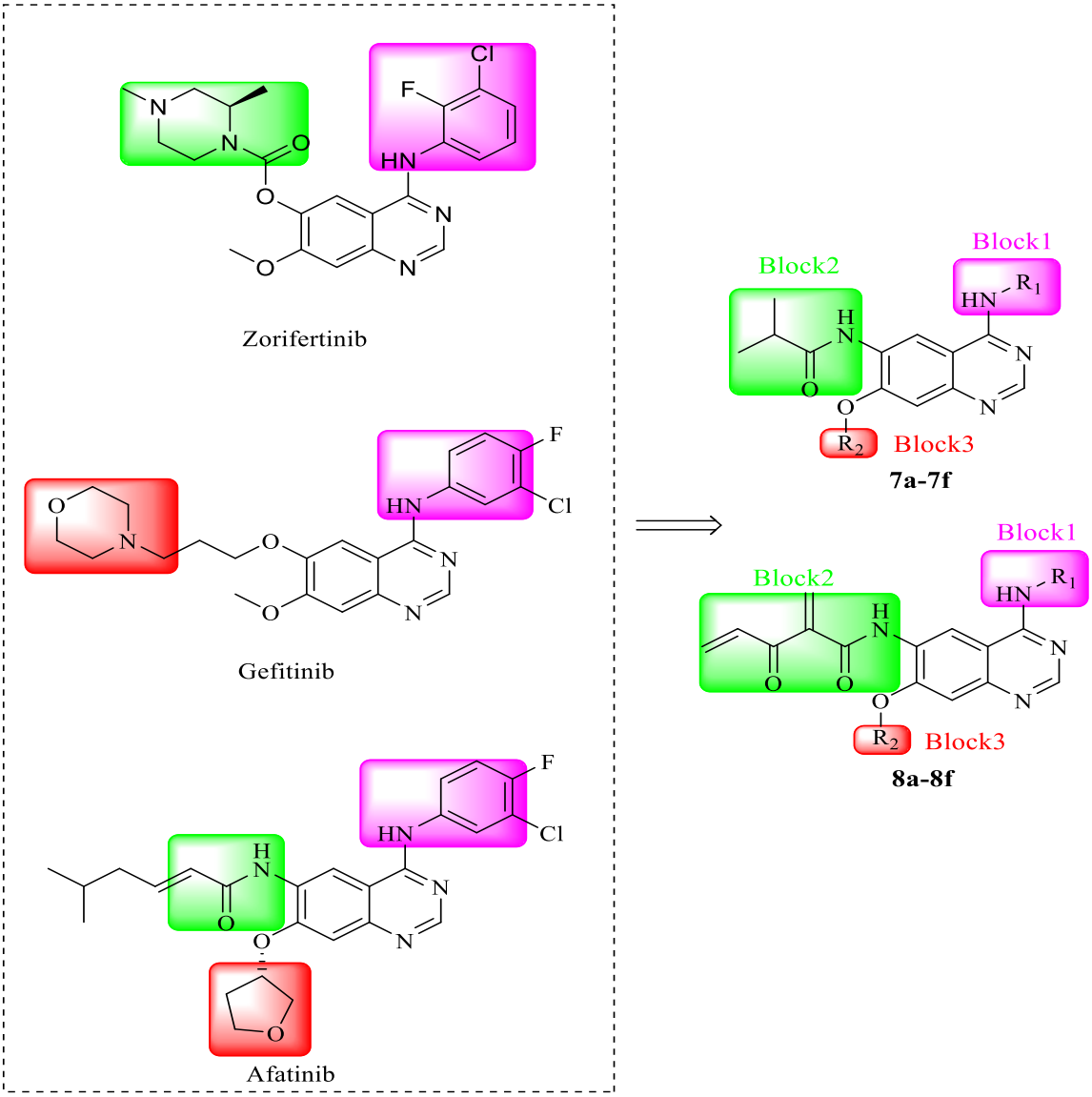

Fig. 2: Design diagram of quinazoline derivatives.

Experiment

Chemistry

General

All chemicals are commercially available and can be used without further purification. The reaction was monitored by TLC (Thin Layer Chromatography) on silica glass plate. The ^{1}HNMR spectra were recorded on a Bruker Biospin 400 MHz or 300 MHz instrument using TMS as internal standard and DMSO-*d6* as solvent; IR spectra were recorded on a Bruker Platinum ART Tensor II FT-IR spectrometer. Mass spectra were acquired on an Esquire-LC mass spectrometer (BrukerDal-tonics, USA) analytical system. The melting point was measured by electron microscope and the thermal melting point meter was not corrected.

General procedure for preparation of 4-(Phenylamino)-7-fluoro-6-nitroquinazoline **(4a-4f)**:

The 7-Fluoro-6-nitroquinazolin-4(3*H*)-one (**1**) (1 g, 4.8 mmol), triethylamine (1.5 mL) and phosphorus oxychloride (1.5 mL) were added to toluene (15 mL). The mixture was stirred at 80 ℃ for 4 h, and monitored by TLC (V_{DCM}: V_{MeOH} = 30 : 1). The next reaction was carried out directly without purification. Compound **3** (4.8 mmol) was added to the reaction solution, and the mixture was heated to 90 ℃ and monitored by TLC (V_{DCM}: V_{MeOH} = 30 : 1). The solid was obtained after the mixture was cooled to 0 ℃, and then was filtered and washed with cold isopropanol. The obtained product was dried in an oven at 40 ℃ for 2 h.

4-(P-methylphenylamino)-7-fluoro-6-nitroquinazoline(**4a**). Yellow solid; Yield 91%; m.p.: 184.6-185.0 ℃; ^{1}H NMR (300 MHz, DMSO-d_6) δ 9.85 (d, J = 7.8 Hz, 1H, Qz/H5'), 8.87 (s, 1H, Qz/H2'), 7.97 (d, J = 11.8 Hz, 1H,-Qz/H8'), 7.77 (d, J = 1.2 Hz, 2H, Bz/H2", H6"), 7.55 – 7.38 (m, 2H, Bz/H3", 5"), 7.31 (t, J = 7.4 Hz, 1H, NH), 2.50 (s, 3H, CH_3); IR (υ_{max}, cm^{-1}) KBr: 3047 (NH), 2361 (CH_3), 1574 (C_{arom}), 1523 (NO_2), 1456 (C_{arom}).

N-(2,4-dimethylphenyl)-7-fluoro-6-nitroquinazolin-4-amine(**4b**). Yellow solid; Yield 93%; m.p.: 176.5-177.9 ℃; ^{1}H NMR (300 MHz, DMSO-d_6) δ 10.64 (s, 1H, Qz/H5'), 9.97 (d, J = 7.7 Hz, 1H, Qz/H2'), 8.80 (s, 1H, NH), 8.05 (d, J = 11.6 Hz, 1H, Qz/H8'), 7.50 – 6.99 (m, 3H, Bz/H3", 5", 6"), 2.33 (s, 3H, CH_3), 2.19 (s, 3H, CH_3); IR (υ_{max}, cm^{-1}) KBr: 3029 (NH), 2959 (CH_3), 1580 (C_{arom}), 1522 (NO_2), 1433 (C_{arom}).

7-Fluoro-N-(2-fluorophenyl)-6-nitroquinazolin-4-amine(**4c**). Yellow solid; Yield 94%; m.p.: 176.3-177.7 ℃; ^{1}H NMR (300 MHz, DMSO-d_6) δ 9.85 (d, J = 7.8 Hz, 1H, Qz/H5'), 8.87 (s, 1H, Qz/H2'), 7.97 (d, J = 11.8 Hz, 1H, Qz/H8'), 7.77 (s, 1H, NH), 7.76 (d, J =6.0 Hz, Bz/H3"), 7.52-7.29 (m, 3H, Bz/H4", H5", H6"); IR (υ_{max}, cm^{-1}) KBr: 3068 (NH), 2952 (CH_3), 1574 (C_{arom}), 1531 (NO_2), 1434 (C_{arom}).

7-Fluoro-N-(4-fluoro-2-methylphenyl)-6-nitroquinazolin-4-amine(**4d**). Yellow solid; Yield 88%; m.p.: 137.3-139.7 ℃; ^{1}H NMR (400 MHz, DMSO-d_6) δ 9.83 (s, 1H, Qz/H5'), 8.81 (s, 1H, Qz/H2'), 8.00 (d, J = 8.2 Hz, 1H, Qz/H8'), 7.38 (s, 1H, NH), 7.30 – 7.02 (m, 3H, Bz/H2", H3", H5"), 2.23 (s, 3H, CH_3); IR (υ_{max}, cm^{-1}) KBr: 3068 (NH), 2960 (CH_3), 1574 (C_{arom}), 1531 (NO_2), 1434 (C_{arom}).

7-Fluoro-6-nitro-N-phenylquinazolin-4-amine(**4e**). Yellow solid; Yield 96%; m.p.: 241.2-242.5 ℃; ^{1}H NMR (400 MHz, DMSO-d_6) δ 10.47 (s, 1H, Qz/H5'), 9.63 (d, J = 6 Hz, 1H, Qz/H2'), 8.68 (s, 1H, Qz/H8'), 7.90 – 7.73 (m, 3H, Bz/H2", H4", H6"), 7.44 (t, J = 7.3 Hz, 2H, Bz/H3", H5"), 7.32 – 7.12 (m, 1H, NH); IR (υ_{max}, cm^{-1}) KBr: 3285 (NH), 2975 (CH_3), 1570 (C_{arom}), 1537 (NO_2), 1412 (C_{arom}).

General procedure for preparation of 7-(Cyclohexyloxy)-N-(substituent)-6-nitroquinazoline-4-amine (**5a-5d**) and *7-(2-Morpholinoethoxy)-6-nitro-N-(substituent) quinazolin-4-amine* (**5e-5h**):

Sodium hydroxide (0.50 g, 20.05 mmol) was added to the mixture of cyclohexanol (1.14 g, 11.41 mmol) (or morpholine ethanol 0.73 g, 5.71 mmol) and tetrahydrofuran (3 mL). The reaction mixture was carried out at room temperature for 2 h. The compound **4** (2.85 mmol) was added and stirred at 40 ℃ for 3 h. After the reaction was completed, the residue was poured directly into ice water and adjusted the pH to 7. The solid (compound **5**) was obtained after filtering and purifying by column chromatography.

7-Cyclohexyloxy-6-nitro-N-(p-tolyl) quinazolin-4-amine(**5a**). Yellow solid; Yield 63%; m.p.: 83.2-84.0 ℃; ^{1}H NMR (400 MHz, DMSO-*d6*) δ 10.00 (s, 1H, Qz/H5'), 9.20 (s, 1H, Qz/H2'), 8.57 (s, 1H, Qz/H8'), 7.68 (d, J = 8.5 Hz, 2H, Bz/H2", H6"), 7.48 (s, 1H, NH), 7.21 (d, J = 8.1 Hz, 2H, Bz/H3", H5"), 4.87 (q, J = 3.0 Hz, 1H, CH), 2.31 (s, 3H, CH_3), 2.12 – 1.03 (m, 10H, CH_2); IR (υ_{max}, cm^{-1}) KBr: 3066 (NH),

2933 (CH_3), 2860 (CH_2), 1567 (C_{arom}), 1522 (NO_2), 1417 (C_{arom}), 1210 (C-O-C).

8-(Cyclohexyloxy)-N-(2,4-dimethylphenyl)-6-nitroquinazolin-4-amine(**5b**). Yellow solid; Yield 65%; m.p.: 77.9-81.2 ℃; ^{1}H NMR (400 MHz, DMSO-d_6) δ 9.92 (s, 1H, Qz/H5'), 9.13 (s, 1H, Qz/H2'), 8.41 (s, 1H, Qz/H8'), 7.48 (s, 1H, NH), 7.19 - 7.07 (m, 2H, Bz/H2", H6"), 7.05 (s, 1H, Bz/H3"), 4.88 (q, J = 3.0 Hz, 1H, CH), 2.31 (s, 3H, CH_3), 2.09 (s, 3H, CH_3), 1.92 (d, J = 6.2 Hz, 2H, CH_2), 1.76 – 1.37 (m, 8H, CH_2); IR (υ_{max}, cm^{-1}) KBr: 3042 (NH), 2945 (CH_3), 2849 (CH_2), 1554 (C_{arom}), 1524 (NO_2), 1436 (C_{arom}), 1240 (C-O-C).

7-(Cyclohexyloxy)-N-(2-fluorophenyl)-6-nitroquinazolin-4-amine(**5c**). Yellow solid; Yield 59%; m.p.: 95.4-96.7 ℃; ^{1}H NMR (300 MHz, DMSO-d_6) δ 10.12 (s, 1H, Qz/H5'), 9.15 (s, 1H, Qz/H2'), 8.51 (s, 1H, Qz/H8'), 7.57 (s, 1H, NH), 7.54 (d, J = 6.2 Hz, 1H, ArH/H4"), 7.33 (m, 3H, Bz/H2", H3", H5"), 4.88 (q, J = 3.0 Hz, 1H, CH), 1.93 (d, J = 12.2 Hz, 2H, CH_2), 1.79 – 1.38 (m, 8H, CH_2). IR (υ_{max}, cm^{-1}) KBr: 3121 (NH), 2930 (CH_3), 2853 (CH_2), 1572 (C_{arom}), 1525 (NO_2), 1421 (C_{arom}), 1235 (C-O-C).

7-(Cyclohexyloxy)-N-(4-fluoro-2-methylphenyl)-6-nitroquinazolin-4-amine(**5d**). Yellow solid; Yield 60%; m.p.: 74.4-77.5 ℃; ^{1}H NMR (300 MHz, DMSO-d_6) δ 9.93 (s, 1H, Qz/H5'), 9.12 (s, 1H, Qz/H2'), 8.41 (s, 1H, Qz/H8'), 7.49 (s, 1H, NH), 7.31 (dd, J = 8.7, 5.6 Hz, 1H, Bz/H2"), 7.17 (dd, J = 9.7, 3.0 Hz, 1H, Bz/H3"), 7.07 (td, J = 8.5, 2.9 Hz, 1H, Bz/H5"), 4.86 (dq, J = 8.2, 4.0 Hz, 1H, CH), 2.16 (s, 3H, CH_3), 1.90 (d, J = 9.9 Hz, 2H, CH_2), 1.75 – 1.56 (m, 4H, CH_2), 1.51 – 1.34 (m, 4H, CH_2). IR (υ_{max}, cm^{-1}) KBr: 3253 (NH), 2934 (CH_3), 2858 (CH_2), 1569 (C_{arom}), 1523 (NO_2), 1420 (C_{arom}), 1230 (C-O-C).

8-(2-Morpholinoethoxy)-6-nitro-N-(p-tolyl) quinazolin-4-amine(**5e**). Yellow solid; Yield 67%; m.p.:98.6-99.8 ℃; ^{1}H NMR (300 MHz, DMSO-d_6) δ 10.01 (s, 1H, Qz/H5'), 9.22 (s, 1H, Qz/H2'), 8.56 (s, 1H, Qz/H8'), 7.71 – 7.62 (m, 2H, Bz/H2", H6"), 7.45 (s, 1H, NH), 7.23 – 7.14 (m, 2H, Bz/H3", H5"), 4.39 (t, J = 5.5 Hz, 2H, OCH_2), 3.54 (d, J = 4.8 Hz, 4H, OCH_2), 2.75 (t, J = 5.5 Hz, 2H, NCH_2), 2.49 – 2.46 (m, 4H, NCH_2), 2.29 (s, 3H, CH_3); IR (υ_{max}, cm^{-1}) KBr: 3339 (NH), 2956 (CH_3), 2808 (CH_2), 1565 (C_{arom}), 1528 (NO_2), 1418 (C_{arom}), 1230 (C-O-Ar), 1104 (C-O-C).

N-(2-fluorophenyl)-7-(2-morpholinoethoxy)-6-nitroquinazolin-4-amine(**5f**). Yellow solid; Yield 64%; m.p.: 73.5-74.9 ℃; ^{1}H NMR (300 MHz, DMSO-d_6) δ 10.17 (s, 1H, Qz/H5'), 9.19 (s, 1H, Qz/H2'), 8.52 (d, J = 2.0 Hz, 1H, Qz/H8'), 7.52 (S, 1H, Bz/H2"), 7.40 – 7.30 (m, 2H, Bz/H3", H5"), 7.27 (dt, J = 9.1, 3.0 Hz, 1H, Bz/H6"), 4.41 (t, J = 4.9, 2.2 Hz, 2H, OCH_2), 3.55 (dt, J = 4.8, 2.8 Hz, 4H, OCH_2), 2.76 (td, J = 5.5, 2.1 Hz, 2H, NCH_2), 2.51 (dd, J = 4.3, 2.1 Hz, 4H, NCH_2); IR (υ_{max}, cm^{-1}) KBr: 3301 (NH), 2937 (CH_3), 2808 (CH_2), 1562 (C_{arom}), 1525 (NO_2), 1409 (C_{arom}), 1238 (C-O-Ar), 1104 (C-O-C).

N-(4-fluoro-2-methylphenyl)-7-(2-morpholinoethoxy)-6-nitroquinazolin-4-amine(**5g**). Yellow solid; Yield 67%; m.p.: 84.2-85.0 ℃; ^{1}H NMR (300 MHz, DMSO-d_6) δ 9.97 (s, 1H, Qz/H5'), 9.14 (s, 1H, Qz/H2'), 8.43 (s, 1H, Qz/H8'), 7.47 (s, 1H, NH), 7.32 (dd, J = 8.7, 5.6 Hz, 1H, Bz/H2"), 7.23 – 7.11 (m, 1H, Bz/H3"), 7.08 (td, J = 8.5, 3.0 Hz, 1H, Bz/H5"), 4.40 (t, J = 5.5 Hz, 2H, OCH_2), 3.55 (d, J = 4.7 Hz, 4H, OCH_2), 2.75 (t, J = 5.5 Hz, 2H, NCH_2), 2.49 – 2.44 (m, 4H, NCH_2), 2.16 (s, 3H, CH_3); IR (υ_{max}, cm^{-1}) KBr: 3145 (NH), 2946 (CH_3), 2817 (CH_2), 1562 (C_{arom}), 1525 (NO_2), 1421 (C_{arom}), 1240 (C-O-ArH), 1109 (C-O-C).

7-(2-Morpholinoethoxy)-6-nitro-N-phenylquinazolin-4-amine(**5h**). Yellow solid; Yield 56%; m.p.: 104.2-105.7 ℃; ^{1}H NMR (300 MHz, DMSO-d_6) δ 10.07 (s, 1H, Qz/H5'), 9.23 (s, 1H, Qz/H2'), 8.59 (s, 1H, Qz/H8'), 7.80 (d, J = 8.0 Hz, 2H, Bz/H2", H6"), 7.47 (s, 1H, NH), 7.39 (t, J = 7.8 Hz, 2H, Bz/H3", H5"), 7.14 (t, J = 7.4 Hz, 1H, Bz/H4"), 4.40 (t, J = 5.5 Hz, 2H, OCH_2), 3.56 (d, J = 4.7 Hz, 4H, OCH_2), 2.76 (t, J = 5.5 Hz, 2H, NCH_2), 2.50 (d, J = 4.3 Hz, 4H, NCH_2); IR (υ_{max}, cm^{-1}) KBr: 3064 (NH), 2963 (CH_3), 2848 (CH_2), 1553 (C_{arom}), 1521 (NO_2), 1445 (C_{arom}), 1267 (C-O-Ar), 1115 (C-O-C).

General procedure for preparation of target compounds **7a-7f** and **8a-8f**:

Compound **5** (3.10 mmol) and zinc powder (1.78 g, 27.40 mmol) were added to the mixture of DCM (10 mL), MeOH (10 mL) and saturated ammonium chloride solution (15 mL). The reaction mixture was carried out at room temperature for 2 h and monitored by TLC (V_{DCM}: V_{MeOH} = 20 : 1). After the reaction was completed, the mixture was concentrated to dryness under reduced pressure and dissolved in DMF (10 mL), then stirred and filtrated to obtain white solid (compound **6**). The compound **6** (1.43 mmol) and triethylamine (0.5 g, 2.34 mmol) were added to THF (15 mL), after stirr at room temperature for 20 min, isobutyryl chloride (0.23 g, 2.14 mmol) or acryloyl chloride (0.38 g, 4.2 mmol)

was added to the reaction which was stirred at room temperature for 3 h, and monitored by TLC (V_{DCM}: V_{MeOH} = 30 : 1). After the reaction was completed, the mixture was concentrated to dryness under reduced pressure, and the obtained solid was filtered and purified by column chromatography to obtain compound **7** and compound **8**.

N-(7-(cyclohexyloxy)-4-(p-tolylamino) quinazolin-6-yl)isobutyramide (**7a**). Yellow solid; Yield 11%; m.p.: 154.2-155.7 ℃; ^{1}H NMR (300 MHz, DMSO-*d6*) δ 9.67 (s, 1H, NH), 9.12 (d, *J* = 3.1 Hz, 1H, Qz/H2'), 8.73 (s, 1H, Qz/H5'), 8.47 (s, 1H, Qz/H8'), 7.79 (s, 1H, NH), 7.37 (t, *J* = 7.9 Hz, 2H, Bz/H2'', H6''), 7.26 (s, 1H, Bz/H5''), 7.18-7.17 (m, 1H, Bz/H3''), 4.68 (t, *J* = 4.0 Hz, 1H, CH), 2.85 – 2.72 (m, 1H, CH), 2.52 (s, 3H, CH_3), 1.97 -1.75 (m, 4H, CH_2), 1.66 – 1.43 (m, 6H, CH_2), 1.19 (s, 3H, CH_3), 1.16 (s, 3H, CH_3); IR (υ_{max}, cm^{-1}) KBr: 3450 (NH), 2922 (CH_2), 2895 (CH), 1667 (C=O), 1527 (C_{arom}), 1445 (C_{arom}), 1260 (C-O-C_{arom}); EIMS: m/z = 419.25 $[M+H]^+$ calculated: 419.24.

N-(7-(cyclohexyloxy)-4-((2,4-dimethylphenyl)amino) quinazolin-6-yl)isobutyramide(**7b**). Brownish yellow solid; Yield 9%; m.p.:181.5-184.1 ℃; ^{1}H NMR (300 MHz, DMSO-d_6) δ 9.44 (s, 1H, NH), 9.09 (s, 1H, Qz/H2'), 8.66 (s, 1H, Qz/H5'), 8.26 (s, 1H, Qz/H8'), 7.22 (s, 1H, NH), 7.07 (d, *J* = 6.2 Hz, 2H, Bz/H2'', H3''), 7.01 (s, 1H, Bz/H5''), 4.64 (s, 1H, CH), 2.83 – 2.74 (m, 1H, CH), 2.30 (s, 3H, CH_3), 2.11 (s, 3H, CH_3), 1.95-1.74 (m, 2H, CH_2), 1.67 (d, *J* = 8.9 Hz, 8H, CH_2), 1.24 – 1.10 (m, 6H, CH_3); IR (υ_{max}, cm^{-1}) KBr: 3501 (NH), 2697 (CH_3), 1659 (C=O), 1505 (C_{arom}), 1448 (C_{arom}), 1234 (C-O-C_{arom}); EIMS: m/z = 433.40 $[M+H]^+$ calculated: 432.25.

O-(7-(cyclohexyloxy)-4-((2-fluorophenyl)amino) quinazolin-6-yl)isobutyramide(**7c**). Yellow solid; Yield 9%; m.p.:144.6-146.3 ℃; ^{1}H NMR (300 MHz, DMSO-d_6) δ 10.08 (s, 1H, NH), 9.26 (s, 1H, Qz/H2'), 8.83 (s, 1H, Qz/H5'), 8.51 (s, 1H, Qz/H8'), 7.55 (t, *J* = 7.8 Hz, 1H, Bz/H2''), 7.39 (d, *J* = 3.7 Hz, 2H, Bz/H3'', H5''), 7.35 (s, 1H, Bz/H4''), 4.73 (s, 1H, CH), 2.91 – 2.84 (m, 1H, CH), 2.04-1.80 (m, 4H, CH_2), 1.74 – 1.54 (m, 4H, CH_2), 1.50 (d, *J* = 13.0 Hz, 2H, CH_2), 1.12 (d, *J* = 1.1 Hz, 3H, CH_3), 1.10 (d, *J* = 1.1 Hz, 3H, CH_3); IR (υ_{max}, cm^{-1}) KBr: 3667 (NH), 2935 (CH_2), 2859 (CH), 1675 (C=O), 1522 (C_{arom}), 1459 (C_{arom}), 1258 (C-O-C_{arom}). EIMS: m/z = 421.20 $[M-H]^+$ calculated: 422.21.

O-(7-(2-morpholinoethoxy)-4-(p-tolylamino)quinazolin-6-yl)isobutyramide(**7d**). Yellow solid; Yield 9%; m.p.:203.1-205.4 ℃; ^{1}H NMR (300 MHz, DMSO-*d6*) δ 9.64 (s, 1H, NH), 8.42 (s, 1H, Qz/H2'), 8.34 (s, 1H, Qz/H5'), 7.30 (s, 1H, Qz/H8'), 7.12 (d, *J* = 5.7 Hz, 3H, Bz/H2'', H5'', H6''), 7.05 (d, 2H ,NH, Bz/H3''), 4.27 (s, 2H, OCH_2), 3.55 (s, 4H, OCH_2), 2.96 (s, 2H, NCH_2), 2.70 (m, 1H, CH), 2.44 (s, 4H, NCH_2), 2.30 (s, 3H, CH_3), 1.07 (s, 6H, CH_3); IR (υ_{max}, cm^{-1}) KBr: 3236 (NH), 2850 (CH_2), 1667 (C=O), 1619 (C=C), 1564 (C_{arom}), 1428 (C_{arom}), 1272 (C-O-C_{arom}). EIMS: m/z = 450.25 $[M+H]^+$ calculated: 450.24.

N-(4-((2-fluorophenyl)amino)-7-(2-morpholinoethoxy)quinazolin-6-yl)isobutyramide(**7e**). Yellow solid; Yield 9%; m.p.:219.7-221.4 ℃; ^{1}H NMR (300 MHz, DMSO-*d6*) δ 9.70 (s, 1H, NH), 9.18 (s, 1H, Qz/H2'), 8.72 (s, 1H, Qz/H5'), 8.35 (s, 1H, Qz/H8'), 7.47 (s, 1H, NH), 7.28 – 7.25 (m, 3H, Bz/H2'', H5'', H6''), 7.18 (d, *J* = 4.0 Hz, 1H, Bz/H3''), 4.31 (t, *J* = 5.5 Hz, 2H, OCH_2), 3.58 (d, *J* = 4.6 Hz, 4H, OCH_2), 2.81 (d, *J* = 7.6 Hz, 2H, NCH_2), 2.48 (s, 4H, NCH_2), 2.32 – 2.27 (m, 1H, CH), 1.16 (s, 3H, CH_3), 1.13 (s, 3H, CH_3); IR (υ_{max}, cm^{-1}) KBr: 3346 (NH), 2922 (CH_2), 2852 (CH), 1665 (C=O), 1625 (C=C), 1577 (C_{arom}), 1424 (C_{arom}), 1254 (C-O-C_{arom}). EIMS: m/z = 476.20 $[M+Na]^+$ calculated: 476.22.

O-(4-((4-fluoro-2-methylphenyl)amino)-7-(2-morpholinoethoxy)quinazolin-6-yl)isobutyramide(**7f**). Yellow solid; Yield 10%; m.p.:224.1-226.4 ℃; ^{1}H NMR (300 MHz, DMSO-*d6*) δ 9.52 (s, 1H, NH), 9.18 (s, 1H, Qz/H2'), 8.69 (s, 1H, Qz/H5'), 8.28 (s, 1H, Qz/H8'), 7.25 (d, *J* = 5.2 Hz, 2H, Bz/H2'', H5''), 7.14 (dd, *J* = 9.8, 3.0 Hz, 1H, NH), 7.04 (td, *J* = 8.6, 3.1 Hz, 1H, Bz/H3''), 4.29 (t, *J* = 5.6 Hz, 2H, OCH_2), 3.58 (d, *J* = 4.6 Hz, 4H, OCH_2), 2.81 (t, *J* = 5.9 Hz, 2H, NCH_2), 2.77 – 2.71 (q, 1H, CH), 2.48 (d, *J* = 1.9 Hz, 4H, NCH_2), 2.13 (s, 3H, CH_3), 1.15 (s, 3H, CH_3), 1.13 (s, 3H, CH_3); IR (υ_{max}, cm^{-1}) KBr: 3226 (NH), 2957 (CH_2), 1667 (C=O), 1625 (C=C), 1579 (C_{arom}), 1421 (C_{arom}), 1240 (C-O-C_{arom}). EIMS: m/z = 490.21 $[M+Na]^+$ calculated: 490.23.

N-(7-(cyclohexyloxy)-4-(p-tolylamino)quinazolin-6-yl)-2-methylene-3-oxopent-4-enamide(**8a**). Yellow solid; Yield 8%; m.p.:201.4-203.8 ℃; ^{1}H NMR (300 MHz, DMSO-d_6) δ 10.44 (s, 1H, NH), 9.04 (s, 1H, Qz/H2'), 8.95 (d, *J* = 8.3 Hz, 1H, Qz/H5'), 7.98 (d, *J* = 11.8 Hz, 1H, Qz/H8'), 7.21 (s, 1H, NH), 7.07 (s, 2H, =CH_2), 6.74 (dd, *J* = 17.0, 10.2 Hz, 1H, =CH), 6.37 (t, *J* = 2.4 Hz, 1H, =CH), 6.31 (dd, *J* = 3.1, 2.0 Hz, 1H, =CH), 6.21 (d, *J* = 10.0 Hz, 1H,

ArH/H2''), 5.87-5.80 (m, 3H, ArH/H3'', 5'', 6''), 2.30-2.24 (m, 4H, CH_2), 2.22 (s, 3H, CH_3), 1.35 – 1.09 (m, 6H, CH_2); IR (υ_{max}, cm^{-1}) KBr: 3479 (NH), 2921 (CH_2), 1680 (C=O), 1619 (C=C), 1563 (C_{arom}), 1451 (C_{arom}), 1273 (C-O-C_{arom}). EIMS: m/z = 455.25 $[M-H]^+$ calculated: 456.22.

O-(7-(cyclohexyloxy)-4-((2-fluorophenyl)amino)quinazolin-6-yl)-2-methylene-3-oxopent-4-enamid(**8b**). Yellow solid; Yield 8%; m.p.:211.3-213.4 ℃; ^{1}H NMR (300 MHz, DMSO-*d6*) δ 9.22 (d, *J* = 2.0 Hz, 1H, NH), 8.14 (d, *J* = 10.8 Hz, 1H, Qz/H2'), 8.07 (d, *J* = 7.7 Hz, 1H, Qz/H2'), 7.47 (s, 1H, NH), 7.41 (s, 1H, Qz/H8'), 7.40 – 7.38 (m, 1H, Bz/H2''), 7.23 (t, *J* = 7.4 Hz, 2H, =CH), 6.53 (s, 1H, Bz/H3''), 6.40 (s, 1H, Bz/H4''), 6.35 (s, 1H, Bz/H5''), 6.22 (d, *J* = 10.6 Hz, 2H, =CH), 5.85 – 5.81 (m, 1H, =CH), 4.26 (td, *J* = 6.2, 2.6 Hz, 1H, CH), 1.43 – 1.27 (m, 2H, CH_2), 1.16 (dd, *J* = 15.7, 8.7 Hz, 4H, CH_2), 0.87 (dd, *J* = 16.8, 9.2 Hz, 4H, CH_2); IR (υ_{max}, cm^{-1}) KBr: 3349 (NH), 2921 (CH_2), 2852 (CH_3), 1690 (C=O), 1623 (C=C), 1563 (C_{arom}), 1458 (C_{arom}), 1259 (C-O-C_{arom}). EIMS: m/z = 461.30 $[M+H]^+$ calculated: 461.19.

N-(7-(cyclohexyloxy)-4-((4-fluoro-2-methylphenyl)amino)quinazolin-6-yl)-2-methylene-3-oxopent-4-enamide(**8c**). Yellow solid; Yield 9%; m.p.:224.1-226.4 ℃; ^{1}H NMR (300 MHz, DMSO-d_6) δ 9.49 (s, 1H, NH), 9.00 (d, *J* = 2.7 Hz, 1H), 8.90 (s, 1H, Qz/H2'), 7.59 (s, 1H, Qz/H5'), 7.40 (d, *J* = 2.9 Hz, 1H, Qz/H8'), 7.31 (dd, *J* = 9.7, 2.7 Hz, 1H, NH), 7.16 – 7.08 (m, 1H, Bz/H2''), 6.83 (dd, *J* = 17.0, 10.2 Hz, 1H, Bz/H3''), 6.39 – 6.32 (m, 2H, =CH), 6.21 (d, *J* = 3.4 Hz, 1H, Bz/H5''), 5.89 – 5.81 (m, 2H, =CH), 4.84 (s, 1H, =CH), 2.35 (s, 3H, CH_3), 2.09-1.81 (m, 4H, CH_2), 1.73 – 1.60 (m, 4H, CH_2), 1.55 – 1.49 (m, 2H, CH_2); IR (υ_{max}, cm^{-1}) KBr: 3407 (NH), 2881 (CH_2), 2659 (CH_3), 1657 (C=O), 1602 (C=C), 1580 (C_{arom}), 1448 (C_{arom}), 1232 (C-O-C_{arom}). EIMS: m/z = 475.30 $[M+H]^+$ calculated: 475.21.

2-Methylene-N-(7-(2-morpholinoethoxy)-4-(phenylamino)quinazolin-6-yl)-3-oxopent-4-enamide(**8d**). Yellow solid; Yield 4%; m.p.:203.1-204.9 ℃; ^{1}H NMR (300 MHz, DMSO-d_6) δ 9.59 (s, 1H, NH), 9.05 (s, 1H, Qz/H2'), 8.93 (s, 1H, Qz/H5'), 7.60 (s, 1H, Qz/H8'NH), 7.43 (h, *J* = 1.2 Hz, 2H, Bz/H2'', H6''), 7.40 (d, *J* = 0.8 Hz, 1H, NH), 7.34 (td, *J* = 3.0, 1.2 Hz, 2H, Bz/H3'', H5''), 6.75 (dd, *J* = 17.0, 10.3 Hz, 1H, Bz/H4''), 6.36 – 6.28 (m, 2H, =CH), 6.27 (dd, *J* = 1.9, 1.0 Hz, 1H, =CH), 5.84 (t, *J* = 1.8 Hz, 1H, =CH), 5.79 (dd, *J* = 3.4, 2.0 Hz, 1H, =CH), 4.44 (t, *J* = 5.9 Hz, 2H, OCH_2), 3.57 – 3.53 (m, 4H, OCH_2), 2.87 (t, *J* = 5.8 Hz, 2H, NCH_2), 2.48 (d, *J* = 1.8 Hz, 4H, NCH_2); IR (υ_{max}, cm^{-1}) KBr: 3086 (NH), 2809 (CH_2), 1665 (C=O), 1619 (C=C), 1525 (C_{arom}), 1440 (C_{arom}), 1217 (C-O-C_{arom}). EIMS: m/z = 475.35 $[M+Na]^+$ calculated: 475.21.

3-Methylene-N-(7-(2-morpholinoethoxy)-4-(p-tolylamino)quinazolin-6-yl)-3-oxopent-4-enamide(**8e**). Yellow solid; Yield 7%; m.p.:212.4-215.1℃; ^{1}H NMR (300 MHz, DMSO-*d6*) δ 10.05 (s, 1H, NH), 9.25 (s, 1H, Qz/H2'), 8.94 (s, 1H, Qz/H5'), 8.59 (s, 1H, NH), 7.69 (s, 1H, Qz/H8'), 7.67 (s, 1H, Bz/H2''), 7.49 (s, 1H, =CH), 7.24 (m, 3H, Bz/H3'', H5'', H6''), 7.20 (s, 1H), 6.98 – 6.55 (m, 1H, =CH), 6.32 (d, *J* = 15.6 Hz, 1H, =CH), 5.81 (dd, *J* = 16.5, 10.4 Hz, 1H, =CH), 3.86 (s, 2H, OCH_2), 3.57 (s, 4H, OCH_2), 2.77 (s, 2H, NCH_2), 2.52 (s, 4H, NCH_2), 2.31 (s, 3H, CH_3); IR (υ_{max}, cm^{-1}) KBr: 3467 (NH), 2856 (CH_2), 1666 (C=O), 1618 (C=C), 1527 (C_{arom}), 1452 (C_{arom}), 1217 (C-O-C_{arom}). EIMS: m/z = 488.30 $[M+Na]^+$ calculated: 488.22.

N-(4-((4-fluoro-2-methylphenyl)amino)-7-(2-morpholinoethoxy)quinazolin-6-yl)-2-methylene-3-oxopent-4-enamide(**8f**). Yellow solid; Yield 8%; m.p.:196.3-198.1℃; ^{1}H NMR (300 MHz, DMSO-*d6*) δ 9.63 (s, 1H, NH), 8.98 (s, 1H, Qz/H2'), 8.86 (s, 1H, Qz/H5'), 7.59 (s, 1H, Qz/H8'), 7.28 (dd, *J* = 9.7, 2.8 Hz, 1H, NH), 7.25 – 7.16 (m, 1H, =CH), 7.09 (dt, *J* = 8.4, 4.1 Hz, 1H, Bz/H2''), 6.78 (dd, *J* = 17.0, 10.2 Hz, 1H, =CH), 6.40 – 6.28 (m, 2H, Bz/H3'', H5''), 6.17 (dd, *J* = 16.7, 10.2 Hz, 1H, =CH), 5.82 (td, *J* = 10.2, 1.8 Hz, 2H, =CH), 4.46 (t, *J* = 6.0 Hz, 2H, OCH_2), 3.59 – 3.55 (m, 4H, OCH_2), 2.89 (t, *J* = 5.8 Hz, 2H, NCH_2), 2.53 (d, *J* = 6.5 Hz, 4H, NCH_2), 2.31 (s, 3H, CH_2); IR (υ_{max}, cm^{-1}) KBr: 3410 (NH), 2924 (CH_2), 2836 (CH), 1735 (C=O), 1614 (C=C), 1581 (C_{arom}), 1431 (C_{arom}), 1212 (C-O-C_{arom}). EIMS: m/z = 523.35 $[M+Na-H]^+$ calculated: 523.23.

CCK-8 assay in vitro

The target compounds (**7a-7f)** and (**8a-8f**) were evaluated against two cancer cell lines (A459 and H1975) by the CCK8 assay, and Afatinib was used as the positive control. The cell suspension was added to a 96-well plate with 1×10^4 cells per well, and they were cultured at 37 ℃ in an incubator containing 5% CO_2. The cell adhesion area was account for 30% of the area of each well, and the prepared solution of the target compound was added into the 96 well plate to to be tested. Then the 96 well plate with the target compound was cultured in the 5% CO_2 incubator at 37 ℃ for 48 h. Then 10 μL CCK solution was added into

each small hole containing cells and was continued to culture in CO_2 incubator for 1-4 h and CCK solution was fully absorbed in the hole. Finally, the absorbance value (OD) of each small hole was measured by microplate reader at 450 nm wavelength. According to the absorbance value, the IC_{50} value of the corresponding compound was calculated and converted by Bliss method. The cell proliferation inhibitor (IR) of each group was calculated by the inhibition rate-absorbance formula. The specific calculation formula was IR% = (control group OD - sample group OD) / (control group OD - blank group OD) × 100%.

Molecular docking study

The protein structures of $EGFR^{WT}$ and $EGFR^{L858R/T790M}$ are retrieved from the RCSB protein database (*RCSB. org*) (PDB IDS: *3w2s* $EGFR^{WT}$ and *5edp* $EGFR^{L858R/T790M}$). They were selected as receptors to study the binding mode with compound **7d**. The preparation steps before docking the receptor protein are as follows: (1) the water molecules in the crystal structure were removed; (2) the pdbqt files of the hydrotreated the receptor protein and ligand structure were generated by autodocktools-1.5.6 (The Scripps Research Institute, La Jolla, California, USA); (3) the protein binding site was covered with a grid box and the most stable mode of docking molecular was selected, and the visual geometric simulation diagram was drawn by PyMOL.

Results and Discussion

Chemistry

The synthetic methods of the target compounds were shown in Fig. 3 [18-22]. 7-Fluoro-6-nitroquinazolin-4(3*H*)-one (**1**) was chlorinated with phosphorus oxychloride to obtain 4-eChloro-7-fluoro-6-nitroquinazoline (**2**). Then intermediate 2 reacted with substituted phenylamine to provide 4-(Substituted phenylamine)-7-fluoro-6-nitroquinazoline (**4**). The intermediate (**4**) was etherified with cyclohexanol or morpholine ethanol to obtain compounds **5a-5h**. Intermediate 6 was provided by the reduction reaction of compound 5, zinc powder and ammonium chloride. Then the compounds **7a-7f** and **8a-8f** were obtained by the acylation of intermediate **6** and acryloyl chloride (or isobutyryl chloride), and their structures were confirmed by ^1H NMR, IR and MS.

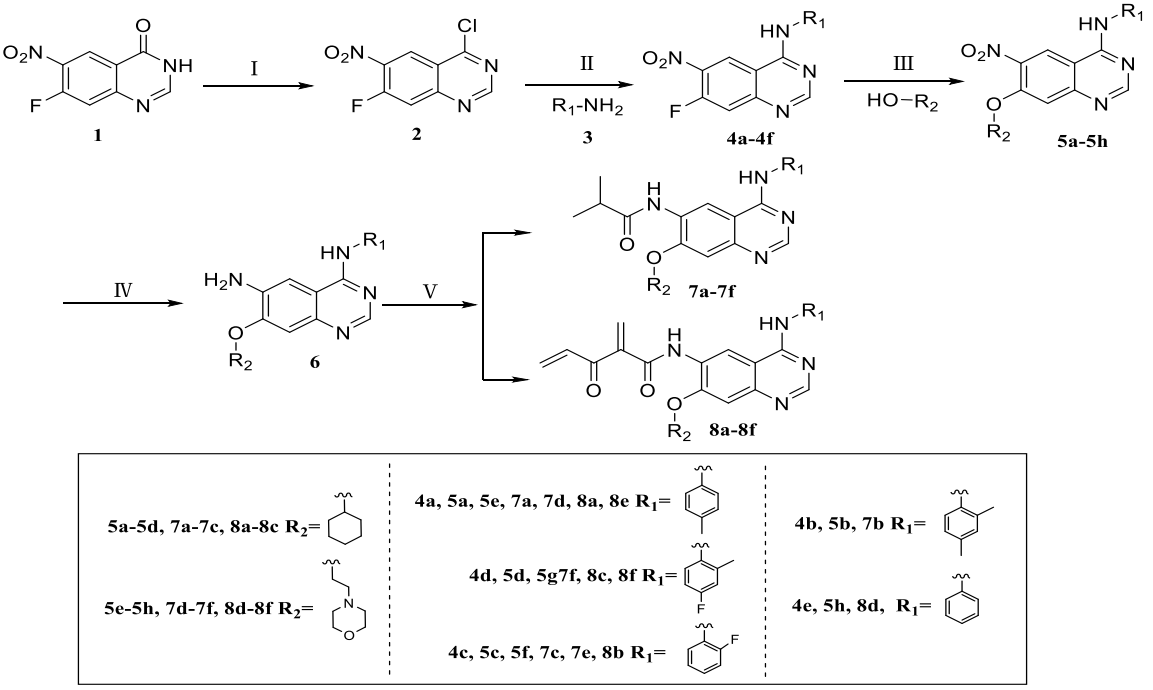

Fig. 3: Synthetic Route of Target Compounds. Reagents and conditions. (Ⅰ) $POCl_3$, toluene, Et_3N at 80 ℃; (Ⅱ) substituted anilines, toluene at 90 ℃; (Ⅲ) Cyclohexanol or Morpholine ethanol, NaH, THF, reflux; (Ⅳ) Zn, NH_4Cl, DCM, MeOH, rt (Ⅴ) acryloyl chloride or isobutyryl chloride, Et_3N, DMF, rt.

In vitro cell activity test Using Afatinib as a positive control, the

synthesized target compounds **7a-7f** and **8a-8f** were tested by CCk-8 analysis for two human lung adenocarcinoma cell lines: A549 (with the overexpressed $EGFR^{WT}$) and H1975 (with the overexpressed $EGFR^{L858R/T790M}$). The results of *in vitro* cytoinhibition rates of the target compounds against A549 and H1975 was shown in Table 1. The results showed that all the tested compounds exhibited excellent anti-tumor activities against the selected cancer cells with cytoinhibition rates ranging from 20.66% to 78.86% for A549, 1.04% to 94.14% for H1975, and it indicated that new synthesized 4-aminoquinazoline derivatives maintained anti-tumor activities. Among these, the compounds **7b**, **7d** and **8f** exhibited remarkable anti-tumor activities against A549 and H1975 cell lines with cytoinhibition rates of 75.94% and 82.97%; 78.86% and 94.14%; 66.85% and 51.25% (Afatinib: 63.86% and 42.26%%). The preliminary structure-activity relationships (SARs) of these compounds exhibited that the cytoinhibition rate of the 7-position of 4-aminoquinazoline replaced by morpholine ethanol group (**7d**: inhibition rate = 78.86% for A549 and inhibition rate = 94.14% for H1975) was better than compound **7a** (which was replaced by cyclohexanol group, inhibition rate = 65.31% for A549 and inhibition rate = 1.04% for H1975), which may be due to the compound with more conducive to transmembrane transport originating from increasing of the lipophilicity and hydrophilicity of the introduction of ethyl morpholine into quinazoline. Meanwhile, the morpholine ring containing nitrogen atoms and oxygen atoms promoted hydrogen bonding and increased the probability of binding between the compound and target protein. In the inhibition rate experiment of human lung cancer cells A549 and H1975, when the benzene ring of 4-aminoquinazoline was replaced by lipophilic groups, the anti-tumor activity of the compounds was enhanced, especially the para and ortho positions of the benzene ring were replaced by methyl (**7b**, inhibition rate = 75.94% for A549 and inhibition rate = 82.97% for H1975; **7d**, inhibition rate = 78.86% for A549 and inhibition rate = 94.14% for H1975). Moreover, the anti-tumor activity of the compounds with large space volume of 4-aniline substituent was significant. It can be assumed that the 4-aniline substituent with large space volume was more suitable for the pore cavity of EGFR protein. It can be seen from Table-1, the introduction of isobutylamide enhanced the anti-tumor activity of the compounds, which may be due to the increasement of the hydrogen bond binding probability between the compounds and the receptor protein. The preferred compounds (**7b** and **7d**) were further evaluated for their *in vitro* inhibitory activities against EGFR kinases of different types (WT and L858R/T790M), and the results were expressed as half-maximal inhibitory concentration (IC_{50}) values. The inhibitory effects of compounds **7b** and **7d** on A549(IC_{50}) and H1975(IC_{50}) were shown in Table 2. The anti-tumor activity of compound **7d** (IC_{50} = 8.35 μM for A549 and IC_{50} = 19.18 μM for H1975) on human lung cancer cells A549 and H1975 was better than Afatinib (IC_{50} = 10.41 μM for A549 and IC_{50} = 24.96 μM for H1975), this may be explained the high affinity between the compound 7d and the two target proteins.

Table-1: In vitro cell inhibition rate of synthesized compounds 7a-7f and 8a-8f.

Comp.	Structure		[a]Inhibition%	
	R_1	R_2	[b]A549	[c]H1975
7a			**65.31**	**1.04**
7b			**75.94**	**82.97**
7c			**20.66**	**73.63**
7d			**78.86**	**94.14**
7e			**24.82**	**27.9**
7f			**55.21**	**43.40**
8a			**52.51**	**39.33**
8b			**47.13**	**36.57**
8c			**48.31**	**47.80**
8d			[d]**n.d**	[d]**n.d**
8e			**40.71**	**64.21**
8f			**66.85**	**51.25**
Afatinib	-	-	**63.86**	**42.26**

[a]Each data represents the average of three different experiments conducted in three repetitions. [b]A549: human lung cancer cell line. [c]H1975: human lung cancer cell line. [d]n.d: not determined

Table-2: In vitro antitumor activity of **7b** and **7d** against different cancer cell lines.

Comp.	Structure	[a]IC_{50} µM	
		[b]A549	[c]H1975
7b	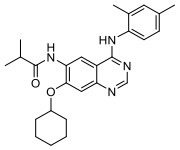	**40.81±0.89**	***n.d**
7d	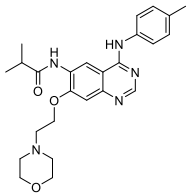	**8.35±1.04**	**19.18±0.93**
Afatinib	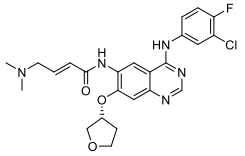	**10.41±0.24**	**24.96±0.25**

[a]IC_{50} values are taken as a mean from three experiments. [b]A549: human lung cancer cell line.
[c]H1975: human lung cancer cell line. *n.d.: not determined.

*Molecular docking of compounds **7d***

A docking assay of compound **7d** and Afitinib with model of EGFRWT protein (PDB Code: *3W2S*)[23] and EGFRL858R/T790M protein (PDB Code: *5EDP*)[24] was simulated using Autodock software, in which Afitinib was used as the original ligand to further explore the relationship between EGFR (WT and L858R/T790M). The docked energy of the derivatives with EGFR kinases are presented in Table-3. The results showed that docked energy data of compound **7d** with Afatinib was comparable. To further elucidate the binding mode of target compound with EGFR kinases of different types (WT and L858R/T790M), the binding mode between compound (**7d**) and EGFR kinase was then proposed by molecular simulation. As shown in the $EGFR^{WT}$ binding model (Fig. 4), the nitrogen atom of quinazoline ring binded to Cys-105 and Asp-108 residues by hydrogen bonds. The oxygen atom of isobutyryl formed a hydrogen bond with Leu-26 residue, and the oxygen atom of morpholine formed a hydrogen bond with Glu-112 residues. In $EGFR^{L858R/T790M}$ binding model, the linked oxygen atom at 7th position of quinazoline formed a hydrogen with Asp-319 and Val-317 residues, which was consistent with previous speculation that the introduction of isobutyryl and morpholinyl enhanced the inhibitory activity of the compounds.

Table-3: Docked energy of compound 7d and Afatinib bound to $EGFR^{WT}$ (PDB code: *3W2S*) and $EGFR^{L858R/T790M}$(PDB code: *5EDP*)

Comp.	Docked energy(kcal/mol)	
	$EGFR^{WT}$	$EGFR^{T790M/L858R}$
7d	**-7.11**	**-7.56**
Afatinib	**-7.73**	**-7.63**

Physicochemical properties and ADME prediction

The partial inhibition rates of selected compounds **7b**, **7d** and **8f** were better than that of the positive control (Afatinib), and used swissADME (a free web tool to evaluate pharmacokinetics, drug likeness and medicinal chemistry friendliness of small molecules) [25-28] to predict the drug properties of the compounds. The prediction results of the compounds were divided into six aspects: lipophilicity (xlogp3), molecular weight, polarity, solubility, flexibility and saturation. The numerical range of the most suitable drug for each physical and chemical property formed a region, as shown in Fig 5. The specific physical and chemical parameters were shown in Table-4, in which all oil-water partition coefficients (log P) are classical descriptors of fat solubility, and the log P of oral drugs is optimal at 0-5. Compound **7b** is 5.12, which may affect its absorption. The MW of compound **8f** violates one of Lipinski's five rules. All compounds had high gastrointestinal absorption and obtained a score of 0.55 in oral utilization. Through the above ADME parameter analysis, the selected compound **7d** had good physical and chemical parameters and had appropriate size in the bioavailability radar map, which is worth to further research and discuss.

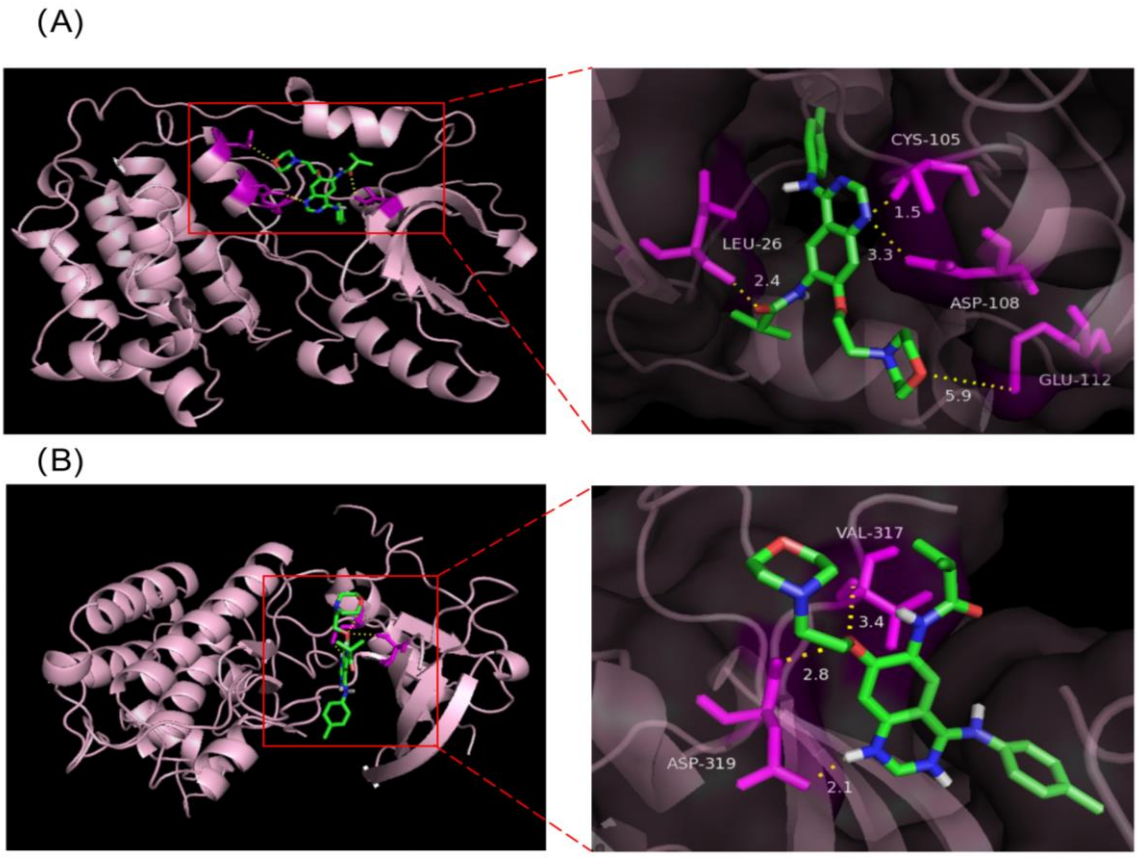

Fig 4: (A) 3D model of compound 7d bound to $EGFR^{WT}$ (PDB code: *3W2S*). (B) 3D model of compound 7d bound to $EGFR^{L858R/T790M}$ (PDB code: *5EDP*).

Fig 5: The Bioavailability Radar enables a first glance at the drug-likeness of the compounds **7b**, **7d** and **8f** afatinib. The pink area represents the optimal range for each properties (lipophilicity: XLOGP3 between −0.7 and +5.0, size: MW between 150 and 500 g/mol, polarity: TPSA between 20 and 130 Å2, solubility: log S not higher than 6, saturation: fraction of carbons in the sp3 hybridization not less than 0.25, and flexibility: no more than 9 rotatable bonds.

Table-4: Physicochemical Properties and ADME Properties of Target Compounds.

Comp.	MW (g/mol) <500	Rotatable bonds	H-bond acceptors <10	H-bond donors <5	TPSA (Å²) ≤140	Log P o/w	[a]Log S	[b]GI	Violation Lipinski Rule of 5	[c]BS
7b	**432.56**	**7**	**4**	**2**	**76.14**	**5.12**	**-6.30**	**high**	**0**	**0.55**
7d	**449.55**	**9**	**6**	**2**	**88.61**	**3.38**	**-4.68**	**high**	**0**	**0.55**
8f	**505.54**	**11**	**8**	**2**	**105.68**	**3.67**	**-5.29**	**high**	**1**	**0.55**
Afatinib	**485.94**	**9**	**7**	**2**	**88.61**	**3.71**	**-4.9**	**high**	**0**	**0.55**

[a]Log S-the water solubility of the compound. [b]GI-gastrointestinal absorption. [c]BS-bioavailability score.

Conclusion

In conclusion, a series of novel 4-aminoquinazoline compounds **7a-7f** and **8a-8f** were designed and synthesized. The synthesized target compounds **7a-7f** and **8a-8f** were tested by CCk-8 analysis for two human lung adenocarcinoma cell lines: A549 (with the overexpressed $EGFR^{WT}$) and H1975 (with the overexpressed $EGFR^{L858R/T790M}$), and Afatinib was used as the positive control. All compounds showed good moderate anti-tumor activity. The anti-tumor activities of compounds **7b**, **7d** and **8f** were better than that of the positive control group. The IC_{50} values of compound **7d** on A549 and H1975 cell lines were 8.35 μM and 19.15 μM respectively, which were better than the Afatinib (IC_{50} = 10.41 μM for A549 and IC_{50} = 24.96 μM for H1975). In addition, we conducted molecular docking and ADME parameter prediction about the compound **7d**, and all these experiments indicated the potential of compound **7d** to develop as potent anti-tumor agent. Further studies on structural optimization and biological activities about these derivatives are still studied in our group and will be reported in the future.

Acknowledgements

This work was supported financially by the Natural Science Foundation of Liaoning Province (NO. 20180550016), the Scientific Research Foundation of the Education Department of Liaoning Province (NO. LJGD2020015).

Conflict of interest

The author(s) declared no potential conflicts of interest with respect to the research, authorship and/or publication of this article.

References

1. X. F. Shang, N. S. L. Morris, Y. Q. Liu, X. Guo, X. S. Xu, M. Goto, J. C. Li, G. Z. Yang, and K. H. Lee, Biologically Active Quinoline and Quinazoline Alkaloids Part I. *Med. Res. Rev.*, **38**, 775(2017).
2. S. I. Leong, J. Schnuerer, and A. Broberg, Verrucine F, A Quinazoline from Penicillium Verrucosum. *J Nat Prod.*, **71**, 1455(2008).
3. A. M. Alafeefy, A. A. Kadi, O. A. Al-Deeb, K. E. H. El-Tahir, and N. A. Al-Jaber, Synthesis, Analgesic and Anti-inflammatory Evaluation of some Novel Quinazoline derivatives. *Eur. J. Med. Chem*., **45**, 4947(2010).
4. V. G. Ugale, S. B. Bari, Quinazolines: New horizons in Anticonvulsant therapy. *Eur. J. Med. Chem*., **80**, 447(2014).
5. D. Xie, J. Shi, A. Zhang, Z. Lei, G. Zu, Y. Fu, X. Gan, L. Yin, B. Song, and D. Hu, Syntheses, Antiviral Activities and Induced resistance mechanisms of Novel Quinazoline derivatives containing a dithioacetal moiety. *Bioorg. Chem*., **80**, 433(2018).
6. A. A. Shalaby, A. M. el-Khamry, S. A. Shiba, A. A. Ahmed, A. A. Hanafi, Synthesis and Antifungal activity of some new Quinazoline and Benzoxazinone derivatives. *Arch. Pharm*., **333**, 365(2000).
7. V. Alagarsamy, K. Chitra, G. Saravanan, V. R. Solomon, M. T. Sulthana, and B. Narendhar, An overview of Quinazolines: Pharmacological Significance and recent developments. *Eur. J. Med. Chem*., **151**, 648(2018).
8. M. U. Rahman, A. Rathore, A. A. Siddiqui, G. Parveen, and M. S. Yar, Synthesis and Characterization of Quinazoline derivatives: Search for Hybrid molecule as diuretic and Antihypertensive agents. *J. Enzyme Inhib. Med. Chem.,* **49**, 733(2014).
9. M. Zengin, O. U. Tan, R. K. Arafa, A. Balkan, Design and Synthesis of new 2-oxoquinoxalinyl-1,2,4-triazoles as antitumor VEGFR-2 inhibitors. *Bioorg Chem*., **121**, 105696(2022).
10. B. Zhang, Z. K. Liu, S. J. Xia, Q. Q. Liu, S. H. Gou, Design, Synthesis and Biological Evaluation of Sulfamoylphenylquinazoline Derivatives as Potential EGFR/CAIX dual inhibitor. *Eur. J. Med. Chem*., **216**, 113300(2021).
11. Z. Q. Cai, Z. S. Jin, D. Q. Zheng, L. Hou, G. W. Huang, J. q. Tian, and G. j. Wang, Synthesis of Several New Quinazolin-4-amines Containing p-toluenesulfonate Moiety. *J. Chem. Res.*, **40**, 573(2016).
12. H. G. Ding, Z. Q. Cai, L. Hou., Z. Q. Hu, Z. S. Jin, D. Xu., H. Cao, M. M. Meng, Y. H. Xie, D. Q. Zheng, Synthesis and Evaluation of Some Novel 6-substituted Quinazoline Derivatives as Antitumor Agents. *J. Chem. Soc. Pak.*, **41**, 186(2019).
13. P. David, AZD3759 for CNS metastases in EGFR-mutant lung cancer[J]. *Lancet. Resp. Med.*, **5**, 841(2017).
14. E. Tsiambas, V. Ragos, A. Y. Lefas, S. N. Georgiannos, D. N. Rigopoulos, G. Georgakopoulos, A. Stamatelopoulos, D. Grapsa and K. Syrigos, Molecular assays in detecting EGFR gene aberrations: an updated HER2-dependent algorithm for interpreting gene signals;

a short technical report[J]. *J. Buon*, **21**, 513(2016).
15. J. Liu, J. Li, J. T. Shi, J. Li, X. C. Hao, D. Z. Song, Y. Wang, S. Ding and Y. Chen, Synthesis and Biological Evaluation of Novel 4-Phenylaminobenzofuro[2,3-d]pyrimidine Derivatives, *J. Chem. Soc. Pak.*, **42**, 564(2020).
16. J. W. Lee, C. Choi, J. Kim, S. H. Lee, J. Kim,Y. J. Lee, K. H. Min. Structure–activity relationships of novel quinazoline derivatives with high selectivity for HER2 over EGFR[J]. *Arch. Pharm. Re*s, **45**, 124 (2022).
17. K. Haider, S. Das, A. Joseph, MS. Yar. An appraisal of anticancer activity with structure–activity relationship of quinazoline and quinazolinone analogues through EGFR and VEGFR inhibition: A review[J]. *Drug. Develop. Res.*, **4**, 83(2022).
18. M. Srinivas, S. Satyaven and B. Ram, Design, Synthesis, and Biological Evaluation of 1,2,4-Oxadiazole-Isoxazole Linked Quinazoline Derivatives as Anticancer Agents. *Russ. J. Gen. Chem*., **89**, 2492(2019).
19. B. Wang, Z. Q. Cai, X. Y. Shi, X. Li, S. Li, and J. X. Li, Synthesis, Crystal Structure and Anticancer Activity of Substituted Quinazoline Derivatives. *J. Chem. Soc. Pak.*, **43**, 466(2021).
20. Z. S Jin, Z. Q. Cai, S. H Fang, R. Zhao, H. G. Ding, H. Cao, D. Xu, M. M. Meng, Y. J. Li, and Q. P. Ma, Study on Synthesis and Antitumor Activities of Novel 4-Substituted Anilinoquinazoline Derivatives. *Chin. J. Synth. Chem*., **26**, 389(2018).
21. J. Liu, Y. L. Gong, J. T. Shi, X. C. Hao, Y. Wang, Y. P. Zhou, Y. L. Hou, Y. J. Liu, S. Ding, Y. Chen, Design, Synthesis and Biological Evaluation of Novel N-[4-(2-fluorophenoxy)pyridin-2-yl] cyclopropanecarboxamide derivatives as potential c-Met Kinase inhibitors. *Eur. J. Med. Chem.*, **194,** 112244(2020).
22. S. Ding, X. Y. Dong, Z. Y. Gao, X. S. Zheng, J. C. Ji, M. J. Zhang, F. Liu, S. G. Wu, W. S. Song, R. Q. Liu, J. W. Shen, J. Liu, Y. Chen, Design, Synthesis and Biological Evaluation of Novel N-(3-amino-4-methoxyphenyl)acrylamide derivatives as selective $EGFR^{L858R/T790M}$ kinase inhibitors, *Bioorg Chem*., **118**, 105471(2022).
23. S. Sogabe, Y. Kawakita and S. Igaki, Structure-Based Approach for the Discovery of Pyrrolo[3,2-d]pyrimidine-Based EGFR T790M/L858R Mutant Inhibitors. ACS. *Med. Chem. Lett*., **4**, 201(2013).
24. J. H. Emily, B. Matt and C. Marian, 4-Aminoindazolyl-dihydrofuro[3,4-d]pyrimidines as non-covalent inhibitors of mutant epidermal growth factor receptor tyrosine kinase. *Bioorg. Med. Chem. Lett*., **26**, 534(2016).
25. A. Daina, O. Michielin and V. Zoete, Swiss ADME: a free web tool to evaluate pharmacokinetics, drug-likeness and medicinal chemistry friendliness of small molecules. *Sci. Rep*.**7**, 2045(2017).
26. A. Daina, O. Michielin and V. Zoete, iLOGP: A Simple, Robust, and Efficient Description of n-Octanol/Water Partition Coefficient for Drug Design Using the GB/SA Approach. *J. Chem. Inf. Mod*., **54**, 3284(2014).
27. C. A. Lipinski, F. B. Lombardo, W. Dominy and P. J. Feeney, Experimental and computationalapproaches to estimate solubility and permeability in drug discovery and development settings. *Adv. Drug Deliv. Rev.*, **23**, 3(1997).
28. D. F. Veber, S. R. Johnson, H. Y. Cheng, B. R. Smith, K. W.Ward and K. D. Kopple, Molecular properties that influence the oral bioavailability of drug candidates. *J. Med. Chem.*, **45**, 2615(2002).